



CHORUS

This is the accepted manuscript made available via CHORUS. The article has been published as:

Vortexlike excitations in the heavy-fermion superconductor CeIrIn_5

Yongkang Luo, P. F. S. Rosa, E. D. Bauer, and J. D. Thompson

Phys. Rev. B **93**, 201102 — Published 5 May 2016

DOI: [10.1103/PhysRevB.93.201102](https://doi.org/10.1103/PhysRevB.93.201102)

Vortex-like excitations in the heavy-fermion superconductor CeIrIn₅

Yongkang Luo,* P. F. S. Rosa, E. D. Bauer, and J. D. Thompson
Los Alamos National Laboratory, Los Alamos, New Mexico 87545, USA.

(Dated: April 21, 2016)

We report a systematic study of temperature- and field-dependent charge (ρ) and entropy (\mathbf{S}) transport in the heavy-fermion superconductor CeIrIn₅. Its large positive thermopower S_{xx} is typical of Ce-based Kondo lattice systems, and strong electronic correlations play an important role in enhancing the Nernst signal S_{xy} . By separating the off-diagonal Peltier coefficient α_{xy} from S_{xy} , we find that α_{xy} becomes positive and greatly enhanced at temperatures well above the bulk T_c . Compared with the non-magnetic analog LaIrIn₅, these results suggest vortex-like excitations in a precursor state to unconventional superconductivity in CeIrIn₅. This study sheds new light on the similarity of heavy-fermion and cuprate superconductors and on the possibility of states not characterized by an order parameter.

PACS numbers: 74.70.Tx, 74.25.fg, 74.25.Uv, 74.72.Kf

Typically, a disorder-order phase transition is described within the context of Ginzburg-Landau theory by an order parameter and identified by a spontaneously broken symmetry. From this point of view, a superconducting transition might be special. The order parameter of superconductivity (SC) is expressed by a complex function in the form $\Psi_s(\mathbf{r})=|\Psi_s(\mathbf{r})|e^{i\theta(\mathbf{r})}$ ¹. Gauge symmetry is broken after phase coherence is established throughout the system. When the phase stiffness is strong, phase coherence develops *concomitantly* as Cooper pairs form, and the superconducting critical temperature T_c is mainly determined by T^{MF} , the mean-field transition temperature predicted by the BCS theory². In contrast, if the superfluid density is small (*e.g.* in underdoped cuprates and organic superconductors), the phase stiffness is low, and the phase coherence can be destroyed by short-lived vortex-like excitations. In this situation, bulk SC cannot be realized until the phases of Cooper pairs are ordered, and T^{MF} is simply the characteristic temperature below which pairing becomes significantly *local* ($T^{MF} \gg T_c$)³. As learned from the cuprates, states without a well-defined order parameter emerge above T_c and include phenomena such as superconducting phase fluctuations, pre-formed Cooper pairs, and a pseudogap.

The CeMIn₅ ($M=\text{Co, Rh and Ir}$) family of tetragonal heavy-fermion compounds is useful platform to investigate the interplay among unconventional SC, antiferromagnetic (AFM) order and spin fluctuations in the vicinity of quantum criticality. The member CeRhIn₅ is an incommensurate antiferromagnet at ambient pressure with Néel temperature $T_N=3.8$ K^{4,5} and can be pressurized into a superconducting state with the highest $T_c \sim 2.2$ K achieved around 2.35 GPa where $T_N(p)$ extrapolates to zero^{6,7}. Textured SC was observed in the region where SC and AFM coexist, characterized by vanishingly small resistivity well above the bulk T_c and the anisotropic resistive T_c ⁸, reminiscent of the nematic state observed in cuprates. In this pressure range, nuclear quadrupole resonance (NQR) experiments suggested the presence of a pseudogap that develops above $T_N(P)$ and extrapolates to the maximum in $T_c(P)$ ⁹. Likewise, scanning tun-

neling spectroscopy revealed a pseudogap that coexists with *d*-wave SC in CeCoIn₅^{10,11}, and replacing a small amount of In by Cd induces coexisting AFM order and SC in CeCo(In_{0.99}Cd_{0.01})₅ where again a transition to zero resistance appears well above the bulk T_c ¹². Pristine CeIrIn₅ shows filamentary SC^{13,14} at atmospheric pressure with a resistive onset temperature $T_c^{on}=1.38$ K, but a diamagnetic state appears only below $T_c^b \simeq 0.5$ K [This is also illustrated in Fig. 1(a)]. Although no direct evidence of magnetic order has yet been identified, chemical substitutions of Hg/Sn on the In site demonstrate that the SC in CeIrIn₅ is in proximity to an AFM quantum-critical point¹⁵. Careful magnetoresistance and Hall effect studies of CeIrIn₅ found evidence for a precursor state of unknown origin arising near 2 K in the limit of zero field^{16,17}. Though the pressure dependence of the precursor state is unknown, the resistive and bulk T_c s approach each other at the maximum in a dome of bulk SC¹⁸, suggesting the possibility that the precursor state may be competing with SC. The complex interplay among states in the CeMIn₅ superconductors bears strikingly similarities to the cuprates, with pure CeIrIn₅ at atmospheric pressure presenting an opportunity to examine more closely these similarities.

From electrical (ρ) and thermoelectric (\mathbf{S}) transport measurements in CeIrIn₅ and a comparison to its non-*4f* counterpart LaIrIn₅, we identify signatures of vortex-like excitations well above T_c^{on} (T_c^b). These findings suggest the existence of a pseudogap-like state where Cooper pairs start to form locally at a temperature well above T_c^{on} , but phase coherence among pairs is destroyed by thermally activated vortex-like excitations, pointing to a common framework for the physics of such states in both heavy-fermion and cuprate¹⁹.

Single crystalline CeIrIn₅ was grown from an indium flux method¹³. The crystal was pre-screened by both resistivity and magnetic susceptibility measurements to ensure the absence of free In. Thermoelectric measurements were carried out by means of a steady-state technique. A pair of well calibrated differential Chromel-Au_{99.93%}Fe_{0.07%} thermocouples was used to measure the

temperature gradient. Upon a thermal gradient $-\nabla T\|\mathbf{x}$ and a magnetic field $\mathbf{B}\|\mathbf{z}$, both thermopower signal $S_{xx}=-E_x/|\nabla T|$ and Nernst signal $S_{xy}=E_y/|\nabla T|$ were collected by scanning field at fixed temperatures. The same contact geometry also was used to measure electrical resistivity (ρ_{xx}) and Hall resistivity (ρ_{yx}). Both electrical and thermal currents were applied along the \mathbf{a} -axis, and the magnetic field was parallel to \mathbf{c} . The same measurements were performed on the non-magnetic analog LaIrIn₅ for comparison. We adopt the sign convention as Ref.²⁰, which defines a *positive* Nernst signal for vortex motion^{21,22}.

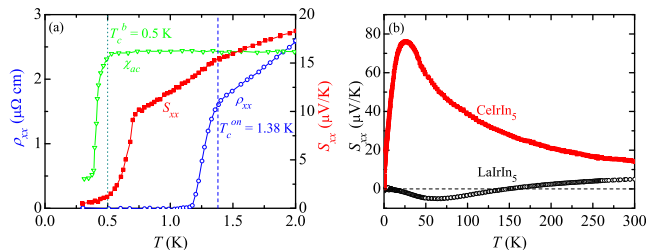


FIG. 1. (Color online) (a) Temperature dependence of ρ_{xx} (blue), χ_{ac} (green) and S_{xx} (red) of CeIrIn₅, showing $T_c^{on}=1.38$ K and $T_c^b=0.5$ K. (b) Comparison of $S_{xx}(T)$ for CeIrIn₅ and LaIrIn₅.

In the presence of a temperature gradient $-\nabla T$, an electric field \mathbf{E} and a magnetic field \mathbf{B} , the total current density is $\mathbf{J}=\boldsymbol{\sigma}\cdot\mathbf{E}+\boldsymbol{\alpha}\cdot(-\nabla T)$, where $\boldsymbol{\sigma}$ is the conductivity tensor, and $\boldsymbol{\alpha}=\frac{\pi^2 k_B^2 T}{3q} \frac{\partial \boldsymbol{\sigma}}{\partial \varepsilon} |_{\varepsilon=\varepsilon_F}$ (k_B is Boltzman constant, q is charge of carriers, ε_F is chemical potential) is the Peltier conductivity tensor²³. In an equilibrium state without net current, the Boltzman-Mott transport equation deduces the thermoelectric tensor

$$\mathbf{S} = \boldsymbol{\alpha} \cdot \boldsymbol{\sigma}^{-1} = \boldsymbol{\alpha} \cdot \boldsymbol{\rho}. \quad (1)$$

We start with the temperature dependence of thermopower $S_{xx}(T)$ as shown in Fig. 1(b). $S_{xx}(T)$ of LaIrIn₅ is positive at room temperature and changes sign near 150 K, characteristic of the expected multi-band behavior²⁴. In contrast, $S_{xx}(T)$ of CeIrIn₅ is positive in the full temperature range between 0.3 K and 300 K, displaying a pronounced maximum at around 25 K with the magnitude reaching 76 $\mu\text{V/K}$. This peak in $S_{xx}(T)$ is associated with the onset of Kondo coherence²⁵. These features are consistent with a Ce-based Kondo lattice in which the strong hybridization between $4f$ - and conduction-electrons forms a Kondo resonance with the density of states $N(\varepsilon)$ asymmetric with respect to ε_F ^{26,27} (see below). At low temperatures, $S_{xx}(T)$ shows a small kink at $T_c^{on}=1.38$ K, but drops sharply at 0.7 K and tends to saturate below $T_c^b=0.5$ K [cf Fig. 1(a)]. Down to the lowest temperature of 0.3 K, however, $S_{xx}(T)$ still remains finite. We attribute this non-vanishing S_{xx} in the bulk superconducting state to the low T_c^b of CeIrIn₅: even

a small temperature gradient may generate ungapped quasiparticles that contribute transport entropy.

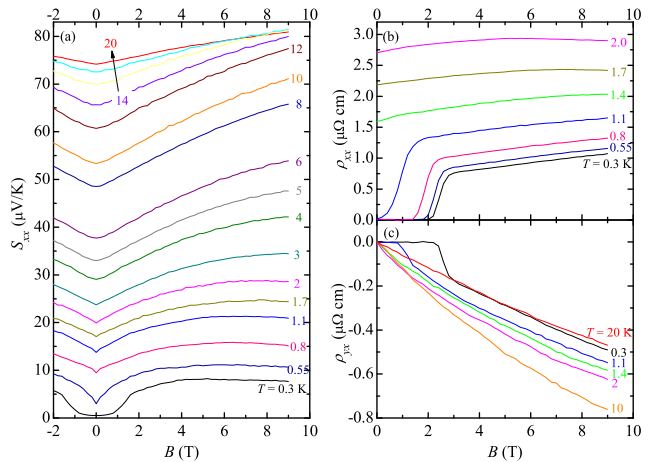


FIG. 2. (Color online) (a) Field dependence of S_{xx} of CeIrIn₅ at selected temperatures. (b) and (c) display $\rho_{xx}(B)$ and $\rho_{yx}(B)$, respectively.

Figure 2(a) displays isothermal field dependence of S_{xx} at various temperatures. For all temperatures, the magneto-thermopower is positive. One important feature of $S_{xx}(B)$ is a valley in the vicinity of zero field. As temperature decreases, this valley deepens and evolves into a cusp when $T \leq 3$ K. At 0.3 K, S_{xx} is small at $B=0$ but recovers when the field is larger than 1.6 T. With the field dependencies of ρ_{xx} and ρ_{yx} shown in Fig. 2(b) and (c), respectively, it is reasonable to attribute this small transport-entropy state to a SC state. The cusp in $S_{xx}(B)$ occurring near 3 K is indicative of the loss of transport entropy well above T_c^b . The critical field recovering a normal state, however, is much smaller than that determined from $\rho_{xx}(B)$ [Fig. 2(b)] and $\rho_{yx}(B)$ [Fig. 2(c)]. Systematic analysis of $\rho_{xx}(B)$ and $\rho_{yx}(B)$ by Nair *et al.*^{16,17} showed that the modified Kohler's scaling $[\Delta\rho_{xx}(B)/\rho_{xx}(0)] \propto \tan^2 \theta_H$, where $\theta_H = \arctan(\rho_{yx}/\rho_{xx})$ is the Hall angle] breaks down prior to T_c^{on} , the region where we observe a large Nernst effect (see below). Similar phenomenon was observed in CeCoIn₅ and CeRhIn₅ under pressure²⁸, as in cuprates, and is reminiscent of a pseudogap-like precursor state²⁹.

In Fig. 3 we present the field dependence of the Nernst signal S_{xy} , the off-diagonal term of the thermoelectric tensor \mathbf{S} . $S_{xy}(B)$ is both negative and linear in B at 20 K. The magnitude of $S_{xy}(B)$ decreases with decreasing T and changes sign near 15 K [Fig. 3(a)]. The non-linearity of $S_{xy}(B)$ becomes pronounced and the value of S_{xy} rapidly increases with decreasing T . At 2 K, S_{xy} reaches 7 $\mu\text{V/K}$ when B is 9 T. We will see that such a large S_{xy} , even larger than that in the vortex-liquid state of cuprates^{21,22}, is mainly due to the Kondo effect, albeit the vortex-like excitation contribution is also non-negligible. A large Nernst effect also has been seen

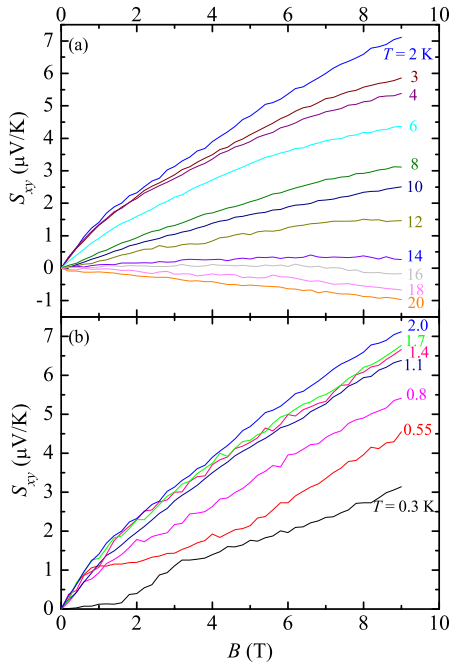


FIG. 3. (Color online) Nernst signal S_{xy} of CeIrIn₅ as a function of B at selected temperatures. (a), $0.3 \leq T \leq 2.0$ K; (b), $2 \leq T \leq 20$ K.

in other Kondo-lattice compounds, like CeCoIn₅^{30–32}, CeCu₂Si₂³³, URu₂Si₂³⁴ and SmB₆³⁵. In CeIrIn₅ S_{xy} starts to drop when T is lower than 2 K but remains positive down to 0.3 K, the base temperature of our measurements [Fig. 3(b)]. At 0.3 K, which is below T_c^b , $S_{xy}(B)$ increases slowly at small field but much more rapidly near 1.8 T. It is likely that this 1.8 T magnetic field defines a melting field B_m above which the vortex solid melts into a vortex-liquid state. A large number of vortices start to move in response to a temperature gradient and this results in the abrupt increase in $S_{xy}(B)$. Similar results also have been seen in other type-II superconductors, like cuprates^{21,22} and CeCoIn₅³¹. This vortex-lattice melting field disappears immediately when T exceeds T_c^b , *e.g.* 0.55 K as shown in Fig. 3(b). This implies that a well-defined Abrikosov-lattice of vortices only exists in the bulk superconducting state of CeIrIn₅.

Figure 4(a) shows the temperature dependence of the Nernst coefficient $\nu_N \equiv S_{xy}/B$. Here, the solid symbols are obtained at $B=9$ T, and the open symbols represent the initial slope of $S_{xy}(B)$ as $B \rightarrow 0$. In both definitions, ν_N above T_c^{on} is large and sign-changes near 15 K. It is well known that for a single-band, non-superconducting and non-magnetic metal, the Nernst signal is vanishingly small, due to so-called Sondheimer cancellation³⁶,

$$S_{xy} = \rho_{xx}\alpha_{xy} - S_{xx} \tan \theta_H. \quad (2)$$

A large Nernst effect has been observed in: (i) multi-band systems such as NbSe₂³⁷ in which the ambipolar effect violates Sondheimer cancellation; (ii) phase slip due to vortex motion in type-II superconductors, as in underdoped

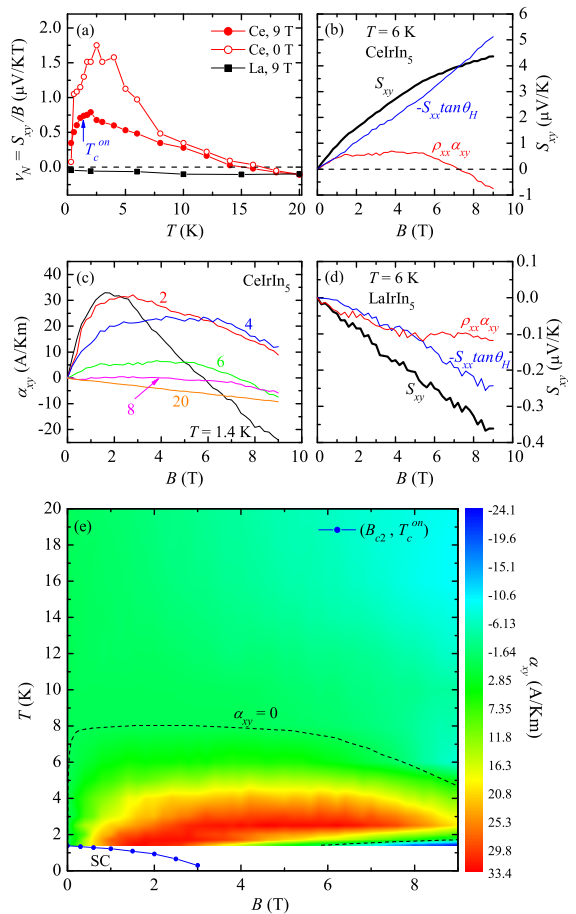


FIG. 4. (Color online) (a) Temperature-dependent Nernst coefficient ν_N of LaIrIn₅ and CeIrIn₅. For CeIrIn₅, the open symbols are the initial slopes of $S_{xy}(B)$ as $B \rightarrow 0$. (b) and (d) show the separation of $\rho_{xx}\alpha_{xy}$ from S_{xy} at $T=6$ K for CeIrIn₅ and LaIrIn₅, respectively. (c) Off-diagonal Peltier coefficient α_{xy} as a function of B at selected temperatures. (e) Contour plot of $\alpha_{xy}(B, T)$, with the resistively determined $B_{c2}(T)$ shown in the lower left corner. The black dash line is the boundary where $\alpha_{xy}=0$.

cuprates^{21,22}; (iii) ferromagnets like CuCr₂Se_{4-x}Br_x in which $S_{xy}(B)$ scales to magnetization $M(B)$, known as anomalous Nernst effect³⁸; (iv) Kondo-lattice systems, like CeCu₂Si₂, in which an enhanced ν_N is determined by asymmetry of the on-site Kondo scattering rate³³.

We can exclude the anomalous Nernst effect in CeIrIn₅ because $S_{xy}(B)$ does not scale with the magnetization, which is essentially a linear function of B (data not shown). From the negative Hall resistivity $\rho_{yx}(B)$ shown in Fig. 2(c), we also rule out a substantive contribution from skew scattering because, as discussed in Refs.^{28,39}, it generates a *positive* anomalous Hall effect for Ce ions.

To study a possible multiband contribution to the Nernst signal of CeIrIn₅, we performed the same measurements on the non-4*f* counterpart LaIrIn₅. According to quantum oscillation measurements and density func-

tional theory (DFT) calculations, LaIrIn₅ is electron-hole compensated^{24,40}, and a large Nernst effect is possible³⁷. The Nernst signal of LaIrIn₅, however, is surprisingly both negative and linear in B [see Fig. 4(d) for instance], and most importantly, the Nernst coefficient remains small between 0.3 K and 20 K [Fig. 4(a)]. This demonstrates that a multiband effect does not play an important role in LaIrIn₅. Compared with LaIrIn₅, CeIrIn₅ has a somewhat larger Fermi surface due to a partially itinerant $4f$ -band²⁴, electron-hole compensation is relatively unbalanced, and, therefore, a multiband contribution to the Nernst signal of CeIrIn₅ is expected to be even weaker.

To better understand the origin of a large Nernst effect in CeIrIn₅, we separate $\rho_{xx}\alpha_{xy}$ from the total Nernst signal S_{xy} [cf Eq. (2)]. As an example, we show S_{xy} , $\rho_{xx}\alpha_{xy}$ as well as $-S_{xx}\tan\theta_H$ at 6 K in Fig. 4(b). As seen, $-S_{xx}\tan\theta_H$ is the dominant contribution to S_{xy} . In a Kondo-lattice system, strong electronic correlations build up a resonance in the density of states near the chemical potential ε_F , and the scattering rate ($1/\tau$) is now mainly determined by the very narrow, renormalized $4f$ -bands, *i.e.* $N_f(\varepsilon)$. As a result, the thermopower, given by Eq. (3), becomes large⁴¹

$$S_{xx} \propto \frac{\partial \ln \tau}{\partial \varepsilon} \propto -\frac{\partial \ln N_f(\varepsilon)}{\partial \varepsilon} \Big|_{\varepsilon=\varepsilon_F} \quad (3)$$

due to an asymmetric $N_f(\varepsilon)$ and is reflected in data plotted in Fig. 1(b). This asymmetry of on-site Kondo scattering also enters S_{xy} through the term $-S_{xx}\tan\theta_H$ and gives rise to the large Nernst effect in CeIrIn₅ and other Kondo-lattice systems as well^{30,31,33,35}.

We note that $-S_{xx}\tan\theta_H$ surpasses S_{xy} when B is larger than 7.3 T at 6 K, and this leads to a sign change in $\rho_{xx}\alpha_{xy}$ [Fig. 4(b)]. Figure 4(c) shows the field dependent α_{xy} at various temperatures. Due to a large contribution from asymmetric Kondo scattering in $S_{xy}(B)$, $\alpha_{xy}(B)$ clearly differs from $S_{xy}(B)$ and, therefore, more intrinsically describes the off-diagonal thermoelectric response. $\alpha_{xy}(B)$ is negative and linear in B at 20 K. As T decreases, an anomalous positive term gradually appears on top of the negative linear background. Similar behavior was observed in CeCoIn₅ and was interpreted as a signature of phase-slip events caused by the passage of individual vortices³¹. To compare, we show $\rho_{xx}\alpha_{xy}$ at 6 K for LaIrIn₅ in Fig. 4(d). As expected, the unusual behavior is absent in LaIrIn₅ where there is only a small negative $\rho_{xx}\alpha_{xy}$.

It is reasonable to write α_{xy} in the form³¹

$$\alpha_{xy} = \alpha_{xy}^n + \alpha_{xy}^s, \quad (4)$$

where α_{xy}^n is the contribution from normal quasiparticles and α_{xy}^s represents an anomalous term stemming from vortex excitations. The positive $\alpha_{xy}(B)$ manifests that vortex motion dominates the quasiparticle term. We summarize these results in a contour plot of $\alpha_{xy}(B, T)$ in Fig. 4(e). Below the $\alpha_{xy}=0$ bound-

ary near 8 K, vortex-like excitations contribute and become most pronounced in the ‘‘island’’ region below 4 K. These temperature scales are qualitatively different from those in CeCoIn₅ in which Nernst effect develops at very low temperature near a field-induced quantum-critical point³². We also note that the temperature dependence of α_{xy}^s/B in CeIrIn₅ cannot be reproduced even approximately by assuming that it arises from Gaussian superconducting fluctuations (data not shown) which seems successful in describing the Nernst effect for optimally-doped and overdoped cuprates but not underdoped ones⁴². Taking $T_c^{on}=1.38$ K in simulation, the calculated α_{xy}^s/B by Gaussian model is an order of magnitude smaller than the observed values. These findings suggest that local Cooper pairs start to form at a temperature well above T_c^{on} and that phase coherence among them is destroyed by thermally activated vortex-like excitations. We estimate the phase-order temperature (above which the phase coherence is destroyed), $T_\theta^{max} \sim 4$ K, if we adopt Emery’s model³ to CeIrIn₅ with lattice parameter $c=7.515 \text{ \AA}$ ¹³ and superconducting penetration depth $\lambda(0) \sim 10^4 \text{ \AA}$ ⁴³. The ratio $T_\theta^{max}/T_c^b \sim 8$ (or $T_\theta^{max}/T_c^{on} \sim 2.9$) is significantly smaller than that of conventional superconductors ($10^2 \sim 10^5$) but is comparable to that of underdoped high- T_c cuprates (<10)³ whose phase stiffness is soft. Perhaps not coincidentally, T_θ^{max} is comparable to the estimated zero-field temperature of a precursor state found in magnetotransport^{16,17}. The filamentary nature of SC¹⁴ also would imply a dilute superfluid density, which renders the phase fluctuations possible in CeIrIn₅³. Finally, we note that the specific heat (C/T) of CeIrIn₅ deviates from a $-\log T$ dependence below ~ 2 -4 K where it rolls over to a weaker (nearly constant) temperature dependence⁴⁴. On a similar temperature scale, ¹¹⁵In nuclear spin-lattice relaxation rate ($1/T_1$) also shows a weak inflection at around 6 K⁴⁵. These evolutions prior to T_c suggest formation of a partial gap in $N(\varepsilon)$ that is in parallel with ungapped heavy quasiparticles. Whether these behaviors are the consequences of a possible pseudogap or correlated with the formation of local Cooper pairs is still an open question and requires further investigation.

Thermoelectric measurements in combination with charge transport in the heavy-fermion superconductor CeIrIn₅ indicate the formation of an unusual state above T_c that is reminiscent of cuprate physics. By separating the off-diagonal Peltier coefficient α_{xy} from S_{xy} , we find that α_{xy} becomes positive and greatly enhanced at the temperatures well above T_c . Compared with the non-magnetic analog LaIrIn₅, these results suggest vortex-like excitations in a precursor state of CeIrIn₅. This work sheds new light on bridging the similarity between heavy-fermion and cuprate superconductors and is a step towards uncovering the mechanism of the unconventional superconductivity in the CeMIn₅ family compounds.

We thank Shizeng Lin for insightful conversations. Work at Los Alamos was performed under the auspices of the U.S. Department of Energy, Division of Materials Sci-

ences and Engineering. P. F. S. Rosa acknowledges sup-

port through a Director's Postdoctoral Fellowship that is funded by the Los Alamos LDRD program.

-
- * ykluo@lanl.gov
- ¹ V. L. Ginzburg and L. D. Landau, *Zh. Eksp. Teor. Fiz.* **20**, 1064 (1950).
 - ² J. Bardeen, L. N. Cooper, and J. R. Schrieffer, *Phys. Rev.* **108**, 1175 (1957).
 - ³ V. J. Emery and S. A. Kivelson, *Nature* **374**, 434 (1995).
 - ⁴ H. Hegger, C. Petrovic, E. G. Moshopoulou, M. F. Hundley, J. L. Sarrao, Z. Fisk, and J. D. Thompson, *Phys. Rev. Lett.* **84**, 4986 (2000).
 - ⁵ W. Bao, P. G. Pagliuso, J. L. Sarrao, J. D. Thompson, Z. Fisk, J. W. Lynn, and R. W. Erwin, *Phys. Rev. B* **62**, R14621 (2000).
 - ⁶ G. Knebel, D. Aoki, D. Braithwaite, B. Salce, and J. Flouquet, *Phys. Rev. B* **74**, 020501 (2006).
 - ⁷ T. Park and J. D. Thompson, *New J. Phys.* **11**, 055062 (2009).
 - ⁸ T. Park, H. Lee, I. Martin, X. Lu, V. A. Sidorov, K. Gofryk, F. Ronning, E. D. Bauer, and J. D. Thompson, *Phys. Rev. Lett.* **108**, 077003 (2012).
 - ⁹ S. Kawasaki, M. Yashima, T. Mito, Y. Kawasaki, G.-q. Zheng, Y. Kitaoka, D. Aoki, Y. Haga, and Y. Onuki, *J. Phys.: Condens. Matter* **17**, S889 (2005).
 - ¹⁰ B. B. Zhou, S. Misra, E. H. da Silva Neto, P. Aynajian, R. E. Baumbach, J. D. Thompson, E. D. Bauer, and A. Yazdani, *Nat. Phys.* **9**, 474 (2013).
 - ¹¹ S. Wirth, Y. Prots, M. Wedel, S. Ernst, S. Kirchner, Z. Fisk, J. D. Thompson, F. Steglich, and Y. Grin, *J. Phys. Soc. Jpn.* **83**, 061009 (2014).
 - ¹² T. Park, X. Lu, H.-O. Lee, and J. D. Thompson, *Physica C* **481**, 223 (2012).
 - ¹³ C. Petrovic, R. Movshovich, M. Jaime, P. G. Pagliuso, M. F. Hundley, J. L. Sarrao, Z. Fisk, and J. D. Thompson, *EPL* **53**, 354 (2001).
 - ¹⁴ A. Bianchi, R. Movshovich, M. Jaime, J. D. Thompson, P. G. Pagliuso, and J. L. Sarrao, *Phys. Rev. B* **64**, 220504 (2001).
 - ¹⁵ T. Shang, R. E. Baumbach, K. Gofryk, F. Ronning, Z. F. Weng, J. L. Zhang, X. Lu, E. D. Bauer, J. D. Thompson, and H. Q. Yuan, *Phys. Rev. B* **89**, 041101 (2014).
 - ¹⁶ S. Nair, S. Wirth, M. Nicklas, J. L. Sarrao, J. D. Thompson, Z. Fisk, and F. Steglich, *Phys. Rev. Lett.* **100**, 137003 (2008).
 - ¹⁷ S. Nair, M. Nicklas, F. Steglich, J. L. Sarrao, J. D. Thompson, A. J. Schofield, and S. Wirth, *Phys. Rev. B* **79**, 094501 (2009).
 - ¹⁸ J. D. Thompson and Z. Fisk, *J. Phys. Soc. Jpn.* **81**, 011002 (2012).
 - ¹⁹ D. J. Scalapino, *Rev. Mod. Phys.* **84**, 1383 (2012).
 - ²⁰ P. W. Bridgman, *Phys. Rev.* **24**, 644 (1924).
 - ²¹ Z. A. Xu, N. P. Ong, Y. Wang, T. Kakeshita, and S. Uchida, *Nature* **406**, 486 (2000).
 - ²² Y. Wang, L. Li, and N. P. Ong, *Phys. Rev. B* **73**, 024510 (2006).
 - ²³ J. M. Ziman, *Electrons and Phonons* (Oxford Clarendon Press, Oxford, 1960).
 - ²⁴ H. Shishido, R. Settai, D. Aoki, S. Ikeda, H. Nakawaki, N. Nakamura, T. Iizuka, Y. Inada, K. Sugiyama, T. Takeuchi *et al.*, *J. Phys. Soc. Jpn.* **71**, 162 (2002).
 - ²⁵ Y. Takaesu, N. Aso, Y. Tamaki, M. Hedo, T. Nakama, K. Uchima, Y. Ishikawa, K. Deguchi, and N. K. Sato, *J. Phys: Conference Series* **273**, 012058 (2011).
 - ²⁶ V. Zlatic and R. Monnier, *Phys. Rev. B* **71**, 165109 (2005).
 - ²⁷ K. Miyake and H. Kohno, *J. Phys. Soc. Jpn.* **74**, 254 (2005).
 - ²⁸ Y. Nakajima, H. Shishido, H. Nakai, T. Shibauchi, K. Behnia, K. Izawa, M. Hedo, Y. Uwatoko, T. Matsumoto, R. Settai *et al.*, *J. Phys. Soc. Jpn.* **76**, 024703 (2007).
 - ²⁹ Y. Abe, K. Segawa, and Y. Ando, *Phys. Rev. B* **60**, R15055 (1999).
 - ³⁰ R. Bel, K. Behnia, Y. Nakajima, K. Izawa, Y. Matsuda, H. Shishido, R. Settai, and Y. Onuki, *Phys. Rev. Lett.* **92**, 217002 (2004).
 - ³¹ Y. Onose, L. Li, C. Petrovic, and N. P. Ong, *EPL* **79**, 17006 (2007).
 - ³² K. Izawa, K. Behnia, Y. Matsuda, H. Shishido, R. Settai, Y. Onuki, and J. Flouquet, *Phys. Rev. Lett.* **99**, 147005 (2007).
 - ³³ P. Sun and F. Steglich, *Phys. Rev. Lett.* **110**, 216408 (2013).
 - ³⁴ T. Yamashita, Y. Shimoyama, Y. Haga, T. D. Matsuda, E. Yamamoto, Y. Onuki, H. Sumiyoshi, S. Fujimoto, A. Levchenko, T. Shibauchi *et al.*, *Nat. Phys.* **11**, 17 (2015).
 - ³⁵ Y. Luo, H. Chen, J. Dai, Z.-a. Xu, and J. D. Thompson, *Phys. Rev. B* **91**, 075130 (2015).
 - ³⁶ E. H. Sondheimer, *Proc. R. Soc. A* **193**, 484 (1948).
 - ³⁷ R. Bel, K. Behnia, and H. Berger, *Phys. Rev. Lett.* **91**, 066602 (2003).
 - ³⁸ W.-L. Lee, S. Watauchi, V. L. Miller, R. J. Cava, and N. P. Ong, *Phys. Rev. Lett.* **93**, 226601 (2004).
 - ³⁹ Y. Luo, F. Ronning, N. Wakeham, X. Lu, T. Park, Z. A. Xu, and J. D. Thompson, *Proc. Natl. Acad. Sci. USA* **112**, 13520 (2015).
 - ⁴⁰ D. Hall, L. Balicas, Z. Fisk, R. G. Goodrich, U. Alver, and J. L. Sarrao, *Phys. Rev. B* **79**, 033106 (2009).
 - ⁴¹ K. Behnia, D. Jaccard, and J. Flouquet, *J. Phys.: Condens. Matter* **16**, 5187 (2004).
 - ⁴² I. Ussishkin, S. L. Sondhi, and D. A. Huse, *Phys. Rev. Lett.* **89**, 287001 (2002).
 - ⁴³ D. Vandervelde, H. Q. Yuan, Y. Onuki, and M. B. Salamon, *Phys. Rev. B* **79**, 212505 (2009).
 - ⁴⁴ R. Borth, E. Lengyel, P. Pagliuso, J. Sarrao, G. Sparn, F. Steglich, and J. Thompson, *Physica B* **312-313**, 136 (2002).
 - ⁴⁵ G.-q. Zheng, K. Tanabe, T. Mito, S. Kawasaki, Y. Kitaoka, D. Aoki, Y. Haga, and Y. Onuki, *Phys. Rev. Lett.* **86**, 4664 (2001).